Onset of Marangoni convection for evaporating liquids with spherical interfaces and finite boundaries

Brendan D. MacDonald and C. A. Ward[*]

Thermodynamics and Kinetics Laboratory, Department of Mechanical and Industrial Engineering, University of Toronto, Toronto, Canada M5S 3G8

We examine the stability of liquids with spherical interfaces evaporating from funnels constructed of different materials. A linear stability analysis predicts stable evaporation for funnels constructed of insulating materials and introduces a stability parameter for funnels constructed of conducting materials. The stability parameter is free of fitting variables since we use the statistical rate theory expression for the evaporation flux. The theoretical predictions are found to be consistent with experimental observations for H_2O evaporating from a funnel constructed of poly(methyl methacrylate) and for H_2O and D_2O evaporating from a funnel constructed of stainless steel.

PACS number(s): 47.20.Dr

I. INTRODUCTION

It has been demonstrated that Marangoni convection can play an important role in transporting thermal energy during evaporation [1–5]. This energy transport is particularly important in applications involving heat transfer at small length scales, such as cooling of microelectronic devices [6]. Also, systems requiring large amounts of heat removal often exploit evaporation since the change-of-phase process involves a significant amount of energy [7,8]. In order to capitalize on the effects of Marangoni convection, an understanding of the onset is needed, but before the onset of Marangoni convection can be understood, certain unresolved issues must be addressed.

We are concerned with three issues in this study: (i) The role of evaporation in the onset of Marangoni convection has not been resolved [9–11], (ii) there are geometrical effects that have not been examined, and (iii) the presence of fitting variables in prediction parameters complicates experimental comparisons. Many studies investigate a semi-infinite sheet in order to isolate the liquid-vapor interface from boundary effects [9]. However, physical systems of interest often have geometries that deviate from semi-infinite sheets. For example, evaporation at the spherical interface of a liquid bounded at a polar angle for all azimuthal angles (i.e., a funnel; see Fig. 1) has been studied experimentally and the conditions at which the liquid makes a transition from a quiescent to a convecting state have been recorded [1,2,4], but none of the presently available stability analyses can be applied to this geometry. Also, in each of these experiments and in others [12], an interfacial temperature discontinuity has been measured in which the interfacial vapor temperature is greater than that of the liquid by several degrees. Fitting variables, such as heat transfer coefficients or the Hertz-Knudsen relation with its evaporation and condensation coefficients, often appear in the stability parameter, which makes it difficult to apply the predictions in an experimental circumstance [11].

The seminal work on Marangoni instability by Pearson [9] involved a linear stability analysis for a semi-infinite sheet. It has been demonstrated that the results are not directly applicable to evaporating systems [4,13,14]. In a recent investigation, evaporation was included in a linear stability analysis [11] for a flat sheet and finite size effects were taken into account by bounding the sheet. The geometry of the system in the funnel experiments [1,2,4] is sufficiently different from flat sheets that a stability analysis is required to explain the observed results. Marangoni convection in evaporating droplets with spherical interfaces has been investigated previously [13,15,16], but the geometry in these studies is for entire spherical droplets with no angular bounding.

In this study we investigate the effect of the funnel material on the stability by performing a linear stability analysis for liquids evaporating from funnels constructed of insulating and conducting materials. We develop the expression for a stability parameter, which provides a quantitative prediction for the transition from a quiescent to a convecting interface for liquids evaporating from funnels constructed of conducting materials. The stability parameter contains no fitting variables since we use the statistical rate theory expression for evaporation flux [11,17]. We compare the theoretical predictions to the experimental observations for H_2O evaporating from a funnel constructed of poly(methyl methacrylate) (PMMA) and for H_2O and D_2O evaporating from a funnel constructed of stainless steel [1,2]. A parametric analysis is performed to show how the stability parameter varies when changing the input quantities.

II. PROBLEM DEFINITION

We investigate a system with an evaporating spherical interface at $r = r_I$ that is bounded at a polar angle of $\pi/4$ by the funnel wall, as shown in Fig. 1. The system is axisymmetric about the $\phi = 0$ centerline. The surrounding fluid is the vapor phase of the liquid and has a temperature at a boundary far from the interface of T_∞. Here the polar angle is given by ϕ as θ is used to denote the temperature perturbation. For the linear stability analysis we perturb the velocity and temperature in the liquid phase and the temperature in the vapor phase. The temperature of the vapor phase is included to ensure a balance of energy and the effect of velocity in the vapor phase is assumed to be negligible.
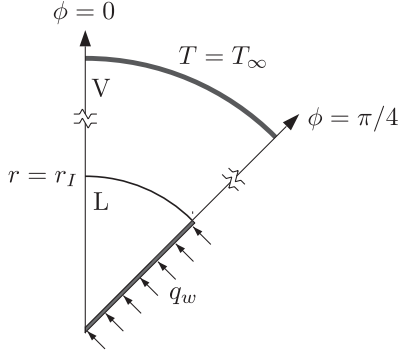
———————
[*]charles.ward@utoronto.ca

FIG. 1. Schematic of the system analyzed in the linear stability analysis.

Typically, investigation of Marangoni instability is for flat sheets, with an interface that is not in contact with a boundary surface, and the temperature gradients normal to the interface generate the instability. However, with a spherical interface bounded in the polar direction, to ensure a stable initial state we require an isothermal liquid phase, thus suppressing tangential temperature gradients along the interface, which would cause Marangoni convection. This assumption is consistent with experimental observations [4]. The initial state therefore requires that the energy necessary for evaporation be provided by conduction through the vapor phase.

III. INITIAL STEADY-STATE SOLUTION

Initially, we consider an evaporating liquid with no Marangoni convection. The initial state is defined based on the stable evaporation observed in the experiments [1,2,4]. Therefore, we have an isothermal liquid phase whereby the energy required for evaporation is provided by conduction through the vapor phase and the vapor phase temperature gradient normal to the interface is uniform along the interface. We assume that the initial evaporation rate is low enough so that the effect of flow through the liquid phase is negligible and the initial velocities are zero. Thus we have

$$\mathbf{U}_{\mathrm{ini}} = \mathbf{0}, \tag{1}$$

$$P_{\mathrm{ini}} = P_0, \tag{2}$$

$$T^L_{\mathrm{ini}} = T_0, \tag{3}$$

$$T^V_{\mathrm{ini}} = T^V_{\mathrm{ini}}(r), \tag{4}$$

where $\mathbf{U}$ is the velocity in the liquid phase, P is the pressure, T is the temperature of either the vapor or liquid phase (superscripts V and L distinguish these), the subscript "ini" denotes the initial state, and a subscript or superscript 0 denotes the initial, unperturbed value of the variable.

With the low flow rate assumption and dependence only in the radial direction, the initial temperature distribution in the vapor phase is governed by the conservation of energy equation

$$\frac{1}{r^2}\frac{\partial}{\partial r}\left(r^2 \frac{\partial T^V_{\mathrm{ini}}}{\partial r}\right) = 0. \tag{5}$$

At $r = r_I$ we have evaporation at a free surface, which yields the energy balance

$$\kappa^V \beta = j_{\mathrm{ev}} h_{fg}, \tag{6}$$

where κ^V is the thermal conductivity of the vapor phase, j_{ev} is the evaporation flux at the interface, and h_{fg} is the enthalpy of vaporization. The uniform vapor phase temperature gradient normal to the interface is denoted by β and the boundary conditions are

$$\left.\frac{\partial T^V_{\mathrm{ini}}}{\partial r}\right|_{r=r_I} = \beta, \tag{7}$$

$$T^V_{\mathrm{ini}}(r \to \infty) = T_\infty. \tag{8}$$

The solution of Eq. (5) with Eq. (7) and Eq. (8) is

$$T^V_{\mathrm{ini}}(r) = T_\infty + \beta\left(-\frac{r_I^2}{r}\right). \tag{9}$$

Now that we have described the initial steady-state solution we can proceed to the linear stability analysis.

IV. LINEAR STABILITY ANALYSIS

In this section we perform a linear stability analysis and derive the equations required to analyze the stability of liquids evaporating from funnels. We perform the analysis for systems with an insulated funnel wall and a conducting funnel wall. The difference between these two analyses is the thermal boundary condition at $\phi = \pi/4$, so we list both of the conditions in the following derivation and provide the analysis for each case independently in the sections that follow.

A. Governing equations

Based on the initial state, we introduce the perturbations

$$\mathbf{U}(r,\phi,t) = \mathbf{u}(r,\phi,t), \tag{10}$$

$$P(r,\phi,t) = P_0 + p(r,\phi,t), \tag{11}$$

$$T^L(r,\phi,t) = T_0 + \theta^L(r,\phi,t), \tag{12}$$

$$T^V(r,\phi,t) = T_\infty + \beta\left(-\frac{r_I^2}{r}\right) + \theta^V(r,\phi,t) \tag{13}$$

and we reiterate that the velocity perturbation and pressure perturbation are for the liquid phase only, so we include no superscript on them. If we use an expression for the evaporation flux j_{ev} from statistical rate theory [17,18], which has no fitting parameters, we can take the derivative with respect to the liquid or vapor temperature. This enables us to write the evaporation flux and enthalpy of vaporization, which are dependent on the liquid and vapor temperatures, as

$$j_{\mathrm{ev}} = j_{\mathrm{ev}}^0 + \frac{\partial j_{\mathrm{ev}}}{\partial T^L}\theta^L + \frac{\partial j_{\mathrm{ev}}}{\partial T^V}\theta^V, \tag{14}$$

$$h_{fg} = \left(h_0^V - h_0^L\right) - c_p^L \theta^L + c_p^V \theta^V, \tag{15}$$

where c_p is the specific heat capacity. The statistical rate theory expression for j_{ev} is listed in the Appendix and a detailed derivation and description can be found in Refs. [17,18].

We introduce the nondimensionalizations

$$r = r^* r_I, \tag{16}$$

$$t = \frac{t^* r_I^2}{\nu}, \tag{17}$$

$$U_r = \frac{U_r^* \alpha}{r_I}, \tag{18}$$

$$U_\phi = \frac{U_\phi^* \alpha}{r_I}, \tag{19}$$

$$P = \frac{P^* \rho \nu \alpha}{r_I^2}, \tag{20}$$

$$T^L = T^{L*} \beta r_I, \tag{21}$$

$$T^V = T^{V*} \beta r_I, \tag{22}$$

where ν is the kinematic viscosity of the liquid, α is the thermal diffusivity, and ρ is the density of the liquid. We assume that the liquid and vapor phases are incompressible and buoyancy effects are negligible (accomplished by exploiting the neutral buoyancy point of water or conditions of near free fall). When the perturbations and scalings are substituted into the conservation equations we have the linearized equations (the asterisk is dropped from the variables and the analysis is nondimensional from here onward)

$$\nabla \cdot \mathbf{u} = 0, \tag{23}$$

$$\frac{\partial \mathbf{u}}{\partial t} = -\nabla p + \nabla^2 \mathbf{u}, \tag{24}$$

$$\mathrm{Pr}\frac{\partial \theta^j}{\partial t} - \nabla^2 \theta^j = 0, \tag{25}$$

where Pr is the Prandtl number (ν/α) and the j superscript is either L for the liquid phase or V for the vapor phase. We can eliminate the pressure term by taking the curl of Eq. (24) twice, yielding

$$\frac{\partial}{\partial t}\nabla^2 \mathbf{u} - \nabla^4 \mathbf{u} = \mathbf{0}. \tag{26}$$

Now that we have a linearized and nondimensional set of governing equations (23), (25), and (26), we can proceed to the linear stability analysis.

B. Marginal stability

The marginally stable state of the system can be described if we assign the following form to the perturbations:

$$u_r = u_{rs}(r,\phi)\exp(\sigma t), \tag{27}$$

$$u_\phi = u_{\phi s}(r,\phi)\exp(\sigma t), \tag{28}$$

$$\theta^L = \theta_s^L(r,\phi)\exp(\sigma t), \tag{29}$$

$$\theta^V = \theta_s^V(r,\phi)\exp(\sigma t), \tag{30}$$

where the s subscript is used to denote the variables corresponding to a state of marginal stability. The governing equations (23), (25), and (26) become, respectively,

$$\nabla \cdot \mathbf{u}_s = 0, \tag{31}$$

$$\sigma \nabla^2 \mathbf{u}_s - \nabla^4 \mathbf{u}_s = \mathbf{0}, \tag{32}$$

$$\mathrm{Pr}\sigma \theta_s^j - \nabla^2 \theta_s^j = 0. \tag{33}$$

We assume the exchange of stabilities is valid, so that σ is real, the marginally stable states are characterized by $\sigma = 0$, and Eqs. (32) and (33) become, respectively,

$$\nabla^4 \mathbf{u}_s = \mathbf{0}, \tag{34}$$

$$\nabla^2 \theta_s^j = 0. \tag{35}$$

At $\phi = \pi/4$, for the insulated funnel wall the conditions are

$$u_{\phi s} = 0, \tag{36}$$

$$-\frac{1}{r}\frac{\partial \theta_s^L}{\partial \phi} = 0. \tag{37}$$

We note that along the funnel wall we allow for slip in the perturbed velocity. For the conducting funnel wall we require an energy balance in the liquid phase between the funnel side wall and evaporation at the liquid-vapor interface, so that instead of Eq. (37) we have

$$\left(\int_0^1 -\frac{1}{r}\frac{\partial \theta_s^L}{\partial \phi} dr \right)_{\phi=\pi/4} = \left(\int_0^{\pi/4} \frac{\partial \theta_s^L}{\partial r} r \, d\phi \right)_{r=1}. \tag{38}$$

At $\phi = 0$ we have an axisymmetric boundary

$$\frac{\partial u_{rs}}{\partial \phi} = 0, \tag{39}$$

$$u_{\phi s} = 0, \tag{40}$$

$$\frac{\partial \theta_s^L}{\partial \phi} = 0. \tag{41}$$

For $r \to \infty$ the vapor phase temperature perturbation satisfies

$$\theta_s^V = 0. \tag{42}$$

At $r = 1$ we have evaporation at a free surface, which is a discontinuous liquid-vapor interface. The boundary conditions can therefore be generated using jump conditions for the balance laws as follows:

$$u_{rs} = \frac{r_I}{\alpha \rho} j_{ev}^0 + \frac{r_I^2 \beta}{\rho \alpha}\left(\frac{\partial j_{ev}}{\partial T^L}\theta_s^L + \frac{\partial j_{ev}}{\partial T^V}\theta_s^V \right), \tag{43}$$

$$\frac{\partial^2 u_{rs}}{\partial r^2} - \frac{\partial^2 u_{rs}}{\partial \phi^2} + 2\frac{\partial u_{rs}}{\partial r} - \cot\phi \frac{\partial u_{rs}}{\partial \phi} - 2u_{rs}$$
$$= -\frac{\gamma_T r_I^2 \beta}{\rho \nu \alpha}\left(\frac{\partial^2 \theta_s^L}{\partial \phi^2} + \cot\phi \frac{\partial \theta_s^L}{\partial \phi} \right), \tag{44}$$

$$\frac{\kappa^V}{\kappa^L}\frac{\partial \theta_s^V}{\partial r} + \frac{r_I}{\kappa^L}\left(-\frac{\partial j_{ev}}{\partial T^V}(h_0^V - h_0^L) - j_{ev}^0 c_p^V \right)\theta_s^V$$
$$= \frac{\partial \theta_s^L}{\partial r} + \frac{r_I}{\kappa^L}\left(\frac{\partial j_{ev}}{\partial T^L}(h_0^V - h_0^L) - j_{ev}^0 c_p^L \right)\theta_s^L, \tag{45}$$

where γ_T is the change of surface tension with respect to temperature and κ is the thermal conductivity of the liquid phase L or vapor phase V. Equation (44) has been simplified to eliminate the dependence on $u_{\phi s}$ by first differentiating by ϕ, then substituting in the continuity equation (31), and finally substituting the undifferentiated initial form to yield the form shown above. With this simplification we require only a solution for u_{rs} in the stability analysis.

For convenience we define the dimensionless groupings from these equations as

$$\xi_C = \frac{r_I}{\alpha\rho} j_{\text{ev}}^0, \tag{46}$$

$$\xi_{CL} = \frac{r_I^2 \beta}{\rho\alpha} \frac{\partial j_{\text{ev}}}{\partial T^L}, \tag{47}$$

$$\xi_{CV} = \frac{r_I^2 \beta}{\rho\alpha} \frac{\partial j_{\text{ev}}}{\partial T^V}, \tag{48}$$

$$\xi_M = \left(-\frac{\gamma_T r_I^2 \beta}{\rho\nu\alpha} \right), \tag{49}$$

$$K = \frac{\kappa^V}{\kappa^L}, \tag{50}$$

$$\xi_{TV} = \frac{r_I}{\kappa^L} \left(-\frac{\partial j_{\text{ev}}}{\partial T^V}\left(h_0^V - h_0^L\right) - j_{\text{ev}}^0 c_p^V \right), \tag{51}$$

$$\xi_{TL} = \frac{r_I}{\kappa^L} \left(\frac{\partial j_{\text{ev}}}{\partial T^L}\left(h_0^V - h_0^L\right) - j_{\text{ev}}^0 c_p^L \right) \tag{52}$$

and note that each of these parameters contains only properties or measurable variables, thus making them physical parameters. Now we can rewrite the conditions at $r = 1$:

$$u_{rs} = \xi_C + \xi_{CL}\theta_s^L + \xi_{CV}\theta_s^V, \tag{53}$$

$$\frac{\partial^2 u_{rs}}{\partial r^2} - \frac{\partial^2 u_{rs}}{\partial\phi^2} + 2\frac{\partial u_{rs}}{\partial r} - \cot\phi\frac{\partial u_{rs}}{\partial\phi} - 2u_{rs}$$
$$= \xi_M \left(\frac{\partial^2 \theta_s^L}{\partial\phi^2} + \cot\phi\frac{\partial\theta_s^L}{\partial\phi} \right), \tag{54}$$

$$K\frac{\partial\theta_s^V}{\partial r} + \xi_{TV}\theta_s^V = \frac{\partial\theta_s^L}{\partial r} + \xi_{TL}\theta_s^L. \tag{55}$$

The term ξ_M in Eq. (54) is traditionally called the Marangoni number. In this analysis we define ξ_M by Eq. (49), so it represents the Marangoni number for a spherical system with an initially isothermal liquid phase and a temperature gradient in the vapor phase. The stability criterion will be developed by substituting the solutions for the velocity and temperature perturbations into Eq. (54) and solving for ξ_M.

The change of phase at the liquid-vapor interface allows us to write a nonzero value for the radial velocity in Eq. (53). The term ξ_C in Eq. (53) is the dimensionless velocity resulting from an evaporation flux. The terms ξ_{CL} and ξ_{CV} relate a temperature change (in the liquid and vapor phases, respectively) to the radial velocity at the interface of an evaporating fluid.

The liquid and vapor phase temperatures are coupled because we include the contributions from both phases in the energy balance of Eq. (55). The physical interpretation of the terms ξ_{TV} and ξ_{TL} is evident from an analogy to the Biot number, since their placement in Eq. (55) indicates they have replaced the Biot number and have the same role. They have eliminated the need for a Biot number since they directly describe the heat transfer conditions at the interface in relation to the evaporation flux. Therefore, the term ξ_{TV} represents the ratio of the resistance to conduction through the vapor phase and the resistance to the evaporation flux at the interface. Likewise, the term ξ_{TL} represents the ratio

of the resistance to conduction through the liquid phase and the resistance to the evaporation flux at the interface. This indicates that higher values for ξ_{TV} and ξ_{TL} correspond to larger temperature gradients building up in the vapor and liquid phases, respectively. Therefore, it is expected that these terms have a crucial role in the stability of the system, as demonstrated by the generation of the stability parameter in Eq. (77), which is listed below.

V. INSULATED FUNNEL WALL

In this section we perform an analysis for liquids evaporating from funnels constructed of insulating materials, using the equations derived above.

A. Liquid phase temperature

We begin with the solution to Laplace's equation (35) for the liquid phase temperature perturbation. The general solution is given as

$$\theta_s^L(r,\phi) = \sum_{n=0}^{\infty}(A_n r^n + B_n r^{-n-1})P_n(\cos\phi), \tag{56}$$

where $P_n(\cos\phi)$ are the Legendre polynomials.

In order for the solution to be bounded at the origin, $B_n = 0$ for all n. We substitute Eq. (56) into Eq. (37) and find

$$-\frac{1}{r}\frac{\partial\theta_s^L}{\partial\phi}\bigg|_{\phi=\pi/4} = \frac{A_1}{\sqrt{2}} + \frac{3A_2}{2}r + \frac{9A_3}{4\sqrt{2}}r^2 + \cdots = 0. \tag{57}$$

Since this expression must equal zero for all values of r, $A_n = 0$ for $n > 0$.

The boundary condition from Eq. (41) is satisfied

$$\frac{\partial\theta_s^L}{\partial\phi}\bigg|_{\phi=0} = 0. \tag{58}$$

The expression for θ_s^L is thus a constant

$$\theta_s^L(r,\phi) = A_0. \tag{59}$$

For the case with an insulated funnel wall, the liquid phase temperature perturbation is constant everywhere. Since the temperature is constant along the free surface, there will be no Marangoni convection and the system is predicted to be stable.

VI. CONDUCTING FUNNEL WALL

In this section we develop an expression to predict the onset of Marangoni convection for liquids evaporating from funnels constructed of conducting materials.

A. Liquid phase temperature

Similar to the analysis above, the general solution to Laplace's equation is Eq. (56) and in order for the solution to be bounded at the origin, $B_n = 0$ for all n. Later in the analysis (Sec. VI D) we will demonstrate that the modes for $n \neq 1$ contribute no valid solutions, so we proceed with the analysis using only the solution for the $n = 1$ mode.

If we consider only the $n = 1$ mode in Eq. (56) and substitute into Eq. (38), we find that both integrals equal

$A_1/\sqrt{2}$, so Eq. (38) is satisfied. The boundary condition from Eq. (41) is also satisfied

$$\left.\frac{\partial \theta_s^L}{\partial \phi}\right|_{\phi=0} = 0. \tag{60}$$

The expression for θ_s^L is

$$\theta_s^L(r,\phi) = A_1 r \cos \phi. \tag{61}$$

The conducting case therefore yields an expression Eq. (61) for the liquid phase temperature perturbation that depends on ϕ, in contrast to the expression for the insulating case Eq. (59).

B. Vapor phase temperature

We now solve for the temperature in the vapor phase. The general solution is

$$\theta_s^V(r,\phi) = \sum_{n=0}^{\infty} (C_n r^n + D_n r^{-n-1}) P_n(\cos \phi). \tag{62}$$

The vapor phase does not include the origin, so we keep the D_n coefficients. Instead we find from the boundary condition at $r \to \infty$ [Eq. (42)], when we substitute in Eq. (62), that $C_n = 0$ for all n. We now substitute into Eq. (55) and find

$$D_1 (\xi_{TV} - 2K) \cos \phi = A_1 (1 + \xi_{TL}) \cos \phi. \tag{63}$$

Therefore, $D_1 = A_1(1 + \xi_{TL})/(\xi_{TV} - 2K)$. The modes for $n \neq 1$ in Eq. (62) cannot produce terms that satisfy the right-hand side of Eq. (63); therefore, $D_n = 0$ for $n \neq 1$.

The expression for θ_s^V is

$$\theta_s^V(r,\phi) = \frac{A_1 \cos \phi}{r^2} \frac{(1 + \xi_{TL})}{(\xi_{TV} - 2K)}. \tag{64}$$

We note that as a result of the coupling in the energy balance Eq. (55), the expressions for both θ_s^L [Eq. (61)] and θ_s^V [Eq. (64)] contain the coefficient A_1. The coefficient A_1 is the only unknown in Eq. (64) since K, ξ_{TV}, and ξ_{TL} are physical parameters, defined in Eqs. (50), (51), and (52), respectively, containing properties or measurable parameters.

C. Liquid phase radial velocity

The general solution to the spherical biharmonic equation (34) is given as [19]

$$u_{rs}(r,\phi) = \sum_{n=0}^{\infty} \left(E_n r^{n+2} + F_n r^n + G_n r^{1-n} \right.$$
$$\left. + H_n r^{-1-n} \right) P_n(\cos \phi). \tag{65}$$

In order for the solution to be bounded at the origin, $G_n = 0$ for $n > 1$ and $H_n = 0$ for all n. The boundary condition from Eq. (39) is satisfied:

$$\left.\frac{\partial u_{rs}}{\partial \phi}\right|_{\phi=0} = 0. \tag{66}$$

We substitute Eq. (65) into Eq. (53) and find

$$(E_0 + F_0 + G_0) + (E_1 + F_1 + G_1) \cos \phi$$
$$= \xi_C + A_1 \left(\xi_{CL} + \frac{\xi_{CV} (1 + \xi_{TL})}{\xi_{TV} - 2K} \right) \cos \phi. \tag{67}$$

Since the modes for $n > 1$ in Eq. (65) have a dependence on $\cos n\phi$, they cannot satisfy the right-hand side of Eq. (67) and must be eliminated. There are no additional boundary conditions to limit which of the coefficients in Eq. (67) are used in the expression for u_{rs}:

$$u_{rs}(r,\phi) = E_0 r^2 + F_0 + G_0 r + (E_1 r^3 + F_1 r + G_1) \cos \phi, \tag{68}$$

so we solve the stability problem considering all of the coefficients and analyze the resulting solutions with respect to their physical validity.

D. Examination of the coefficients

In order to derive the stability criterion we rearrange Eq. (54) and add the s subscript to distinguish the result of the stability analysis from the physical definition of ξ_M given above in Eq. (49):

$$\xi_{Ms} = \frac{\frac{\partial^2 u_{rs}}{\partial r^2} - \frac{\partial^2 u_{rs}}{\partial \phi^2} + 2\frac{\partial u_{rs}}{\partial r} - \cot \phi \frac{\partial u_{rs}}{\partial \phi} - 2u_{rs}}{\frac{\partial^2 \theta_s^L}{\partial \phi^2} + \cot \phi \frac{\partial \theta_s^L}{\partial \phi}}. \tag{69}$$

Substituting in the solutions for θ_s^L [Eq. (61)], θ_s^V [Eq. (64)], and u_{rs} [Eq. (68)] yields

$$\xi_{Ms} = \frac{1}{A_1} \left(-\frac{2E_0}{\cos \phi} + \frac{F_0}{\cos \phi} - 6E_1 - F_1 \right). \tag{70}$$

We can see from Eq. (70) that the E_0 and F_0 coefficients result in terms that generate a ϕ dependence for ξ_{Ms}. From Eq. (49) we can see that ξ_M contains no terms with a dependence on ϕ. In order to satisfy Eq. (54), ξ_{Ms} must be set equal to ξ_M, so ξ_{Ms} must also have no dependence on ϕ. Therefore, $E_0 = 0$, $F_0 = 0$, and, in order to satisfy Eq. (67), $G_0 = \xi_{C1}$.

We investigate the remaining coefficients in Eq. (70) individually. If we use G_1 to solve Eq. (67), the resulting ξ_{Ms} expression would be zero and there would be no onset prediction. Therefore, we set $G_1 = 0$. There are two remaining cases: We can either solve Eq. (67) for E_1 and set F_1 equal to zero (case E_1) or solve for F_1 and set E_1 equal to zero (case F_1). Utilizing combinations of these terms would result in a description of the stability parameter with ambiguous constants, which would have to be eliminated, so we consider only these two cases. For case E_1 we find

$$\xi_{Ms}^{E_1} = -6 \left(\xi_{CL} + \frac{\xi_{CV} (1 + \xi_{TL})}{\xi_{TV} - 2K} \right) \tag{71}$$

and for case F_1 we find

$$\xi_{Ms}^{F_1} = -\left(\xi_{CL} + \frac{\xi_{CV} (1 + \xi_{TL})}{\xi_{TV} - 2K} \right). \tag{72}$$

The form given in Eq. (72) is a multiple of Eq. (71), so we can analyze only Eq. (71) since the $1/6$ multiplier applied to ξ_M corresponds to the least stable case.

We elaborate here on the exclusion of all modes except the $n = 1$ mode for the liquid phase temperature solution. Similar to the argument for eliminating the E_0 and F_0 coefficients above, we found that utilizing higher modes in the solution for θ_s^L only yields additional terms in ξ_{Ms} that are dependent on ϕ. Since we can have no ϕ dependence in ξ_{Ms} we can consider only the form of θ_s^L for the $n = 1$ mode, given in Eq. (61).

E. Stability parameter for a conducting funnel wall

To examine the stability we equate the result from the perturbation analysis Eq. (71) and the physical definition of ξ_M from Eq. (49):

$$-6\left(\xi_{CL} + \frac{\xi_{CV}(1+\xi_{TL})}{\xi_{TV} - 2K}\right) = \xi_M. \quad (73)$$

We substitute in Eqs. (47), (48), and (49) and rearrange terms

$$-\frac{r_I^2\beta}{\rho\alpha}\left[\left.\frac{\partial j_{\mathrm{ev}}}{\partial T^L}\right|_I + \left.\frac{\partial j_{\mathrm{ev}}}{\partial T^V}\right|_I\left(\frac{1+\xi_{TL}}{\xi_{TV} - 2K}\right)\right] = -\frac{1}{6}\frac{\gamma_T r_I^2\beta}{\rho\nu\alpha}. \quad (74)$$

The terms ξ_{TL} and ξ_{TV} were not substituted for since no simplification results from the substitution. We cancel the terms common to both sides of the equation and obtain

$$-\left[\left.\frac{\partial j_{\mathrm{ev}}}{\partial T^L}\right|_I + \left.\frac{\partial j_{\mathrm{ev}}}{\partial T^V}\right|_I\left(\frac{1+\xi_{TL}}{\xi_{TV} - 2K}\right)\right] = -\frac{1}{6}\frac{\gamma_T}{\nu}. \quad (75)$$

We now have an expression that relates the evaporation properties of the fluid to the ratio between the surface tension forces and viscous forces. In order to generate a stability parameter that is dimensionless we rearrange Eq. (75) as

$$\frac{\nu}{\gamma_T}\left[\left.\frac{\partial j_{\mathrm{ev}}}{\partial T^L}\right|_I + \left.\frac{\partial j_{\mathrm{ev}}}{\partial T^V}\right|_I\left(\frac{1+\xi_{TL}}{\xi_{TV} - 2K}\right)\right] = \frac{1}{6}. \quad (76)$$

We define the stability parameter χ_s as the left-hand side of Eq. (76):

$$\chi_s = \frac{\nu}{\gamma_T}\left[\left.\frac{\partial j_{\mathrm{ev}}}{\partial T^L}\right|_I + \left.\frac{\partial j_{\mathrm{ev}}}{\partial T^V}\right|_I\left(\frac{1+\xi_{TL}}{\xi_{TV} - 2K}\right)\right]. \quad (77)$$

We note that χ_s is comprised entirely of physical variables that are either properties or parameters that can be measured, so we can compare this expression directly with experimental observations. In contrast to the conventional stability investigations for nonvolatile fluids and semi-infinite systems, the stability parameter does not depend on temperature gradients since β was canceled in Eq. (74). Therefore, the expression for the stability parameter is instead a function of the conditions at the interface. We also note the importance of including the vapor phase thermal contributions in the interfacial energy balance Eq. (55) since the vapor phase contributions are present in the stability parameter, particularly the term K, which is the ratio of thermal conductivity of the vapor and liquid phases.

VII. EXPERIMENTAL RESULTS

In this section we compare the theoretical predictions to the experimental observations [1,2,4]. We note that the liquid phase in these experiments was isothermal prior to the onset of Marangoni convection. Since there were no temperature gradients in the liquid phase, there could not have been any buoyancy-driven convection; hence, the observed transition to convection was the result of surface tension effects.

A. Experiments with a PMMA funnel

For liquids evaporating from funnels constructed of an insulating material, the theoretical analysis in Sec. V predicts that there will be no Marangoni convection and the system is stable. In the experiments of Ref. [4], H_2O was evaporating

from a funnel constructed of PMMA. Since the thermal conductivity of PMMA is less than one-third that of water, the funnel is considered to be insulating. In these experiments the system was observed to be stable and there were no conditions in the investigation whereby Marangoni convection could be initiated. Therefore, the theoretical result correctly describes the observations in the experiments [4].

B. Experiments with a stainless steel funnel

We will now compare the predictions for a transition to Marangoni convection calculated with the stability parameter derived in Sec. VI to the experimental results with H_2O and D_2O evaporating from funnels constructed of stainless steel [1,2]. The values measured during the D_2O experiments [2] are listed in Table I. In experiments EVD1 through EVD4, quiescent (stable) evaporation was observed as the evaporation rate was progressively increased from one experiment to the next. Experiment EVD5 was the first in which a convecting state was observed. Thus we expect a transition to Marangoni convection to occur between EVD4 and EVD5.

Similarly, the values measured during the H_2O experiments [1] are listed in Table II. In experiments EV5 through EV7, quiescent (stable) evaporation was observed as the evaporation rate was increased. EV8 was the first experiment where a convecting state was observed, so we expect a transition to occur between EV7 and EV8 for the H_2O experiments.

The interfacial radius r_I listed in Tables I and II is the radius shown in Fig. 1, which was calculated based on the geometry such that the funnel wall corresponded to the origin of the spherical coordinate system and was located at an angle of $\pi/4$. This is an approximation, which differs from the interface radius reported in Ref. [2] because that radius was calculated for a different purpose by considering the curvature of the interface and not for the location of the funnel wall. The difference between these two values results in a negligible change for the calculations performed in this analysis.

The interfacial vapor phase temperature T_I^V listed in Tables I and II is labeled as the extrapolated value. The T_I^V values reported in the experiments of Refs. [1,2] correspond to a temperature measurement that is approximately 40 μm away from the interface (in the normal direction). This is a result of the bead diameter of the thermocouple (approximately

TABLE I. Conditions for the D_2O experiments [2]. The extrapolated value is denoted by "extrap."

	Experiment		
	EVD1	EVD4	EVD5
P^V (Pa)	651.9 ± 13.3	642.6 ± 13.3	625.3 ± 13.3
r_I (mm)	4.4 ± 0.01	4.4 ± 0.01	4.4 ± 0.01
j_{ev} (g/m^2 s)	0.059 ± 0.001	0.089 ± 0.001	0.221 ± 0.002
throat T^L (°C)	3.60 ± 0.02	3.58 ± 0.02	3.61 ± 0.02
extrap. T_I^V (°C)	4.41 ± 0.64	4.33 ± 0.64	4.04 ± 0.64
onset χ_s	0.167	0.167	0.167
onset T_I^V (°C)	3.641	3.621	3.652
interface observed	quiescent	quiescent	convection
prediction	quiescent	quiescent	possible convection

TABLE II. Conditions for the H_2O experiments [1].

	Experiment		
	EV5	EV7	EV8
P^V (Pa)	787.9 ± 13.3	783.9 ± 13.3	777.3 ± 13.3
r_I (mm)	4.4 ± 0.01	4.4 ± 0.01	4.4 ± 0.01
j_{ev} (g/m^2 s)	0.057 ± 0.001	0.070 ± 0.001	0.100 ± 0.002
throat T^L (°C)	3.56 ± 0.03	3.53 ± 0.03	3.53 ± 0.03
extrap. T_I^V (°C)	4.42 ± 0.64	4.31 ± 0.64	4.23 ± 0.64
onset χ_s	0.167	0.167	0.167
onset T_I^V (°C)	3.625	3.595	3.595
interface observed	quiescent	quiescent	convection
prediction	quiescent	quiescent	possible convection

50 μm), the gap required to ensure the bead was not in contact with the liquid phase, and the accuracy of the cathetometer used for positioning (± 10 μm). The stability is sensitive to the value of T_I^V, so we require the value at the interface and an understanding of its uncertainty range. The temperature measurements were made as close to the interface as possible (thermocouple bead located 40 μm away) and at regular intervals progressively further from the interface (in a direction normal to the interface). We use these data points to generate a fit and extrapolate to the interface. The fit corresponds to the solution for the vapor phase temperature in the initial stable state reported above as Eq. (9). We find values for T_∞ and β and list these in Table III for each experiment. An example of the measured data points and the fit are plotted in Fig. 2 for experiment EV8 to elucidate the method, results, and estimated error.

The estimated error range listed in Tables I and II for the extrapolated T_I^V values is a result of the temperature measurement inaccuracy, the uncertainty in the interface location, and the fitting and extrapolation errors. The cathetometer uncertainty of ± 10 μm leads to an uncertainty of ± 20 μm in the location of the interface since both the steady-state position of the interface, where evaporation is taking place, and the thermocouple bead location rely on positioning performed with the cathetometer. Although the temperature measurement inaccuracy is ± 0.02 °C, the combination of bead and interface location uncertainty, and the fitting and extrapolation errors raises the estimated error to $\pm$ 0.64 °C.

The stability parameter χ_s is a function of the interfacial liquid and vapor temperatures, the vapor phase pressure of the system, and the radius of the spherical interface. The expression for the evaporation flux j_{ev} derived from

TABLE III. Coefficients for the T^V fit using Eq. (9).

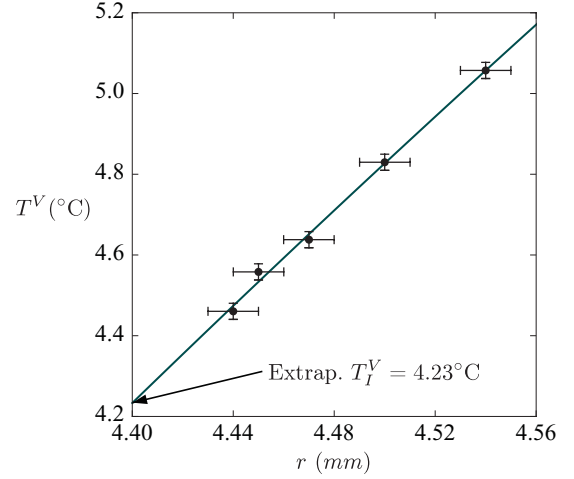|	Coefficient	
Experiment	T_∞ (°C)	β (°C/m)
EVD1	28.75 ± 1.97	5531 ± 456
EVD4	26.73 ± 2.04	5091 ± 474
EVD5	26.07 ± 0.93	5006 ± 216
EV5	33.46 ± 1.38	6601 ± 319
EV7	30.55 ± 0.72	5963 ± 167
EV8	30.95 ± 1.01	6071 ± 233

FIG. 2. (Color online) Plot of the experimental data (points) and the fit (solid line) for the vapor phase temperatures in the EV8 experiment. The interface is located at $r = r_I = 4.40$ mm.

statistical rate theory is sensitive to values of the vapor phase pressure [17]. The equipment provided a measurement range of ± 13.3 Pa, which is not accurate enough to predict j_{ev}. However, the evaporation rate was measured with a syringe pump for these experiments. So instead of calculating the value of j_{ev} from the experimental measurements, we can insert the value directly and investigate the stability parameter as a function of the evaporation flux also:

$$\chi_s = \chi_s\big(j_{ev}^0, T_I^V, T_I^L, P^V, r_I\big). \quad (78)$$

Once the evaporation flux is inserted directly into the calculation of χ_s, the effect of the vapor phase pressure on the values of χ_s becomes negligible. The derivative of the evaporation flux with respect to the liquid or vapor temperature, required for Eq. (77), can be calculated using an expression for the evaporation flux j_{ev} from statistical rate theory [17,18] [Eq. (A1)], which has no fitting parameters, as noted above. The derivatives are not sensitive to the vapor phase pressure values and can be calculated from the expression.

C. Stability prediction for the D_2O experiments

We determine if the stability parameter χ_s predicts the transition to Marangoni convection observed in the experiments of Ref. [2]. The fluid used in this study was D_2O and we use the properties given in Ref. [2]. The right-hand side of Eq. (76) corresponds to the onset value of 1/6 (0.167).

If we calculate the value of χ_s directly from the experimental values listed in Table I, without considering the uncertainty ranges, we find that the value of χ_s is less than the onset value (0.167) and the system is predicted to be stable for all of the experiments. However, we need to determine if an instability is predicted to occur within the uncertainty ranges of the experimental data. Since T_I^V has the largest uncertainty range, we examine it first while holding the other experimental parameters in Eq. (78) constant and calculate the value that would be required for the onset of an instability.

The results of the investigation are summarized in Table I. We find that the instability is predicted to occur at a T_I^V value of approximately 3.641°C for EVD1, 3.621°C for EVD4, and 3.652 °C for EVD5. The onset T_I^V value for EVD5, in which Marangoni convection was observed, lies within the possible range; however, the values for EVD1 and EVD4, which were observed to be quiescent, do not lie within the possible range. The uncertainty ranges for j_{ev} and T_I^L were also investigated and there were no values within the ranges that predicted an instability for EVD1 and EVD4. Therefore, the theory is consistent with experimental observations since it predicts that a transition to Marangoni convection is possible between EVD4 and EVD5.

D. Stability prediction for the H_2O experiments

We determine if the stability parameter predicts the transition to Marangoni convection observed in the experiments of Ref. [1]. The fluid used in this study was H_2O and we use the properties listed in Ref. [1].

Similar to the D_2O case, if we calculate the value of χ_s directly from the experimental values listed in Table II, without considering the uncertainty ranges, we find that the value of χ_s is less than the onset value (0.167) and the system is predicted to be stable for all of the experiments. As we did above, we determine if an instability is predicted to occur within the uncertainty ranges of the experimental data, beginning with an investigation of T_I^V while holding the other experimental parameters in Eq. (78) constant and calculating the value that would be required for the onset of an instability.

We find that the predicted T_I^V values are outside the uncertainty ranges for fixed values of j_{ev} and T_I^L. If we allow T_I^L to vary within the uncertainty range, we find that for the highest values of T_I^L (0.03 °C above the values listed in Table II) the predicted T_I^V values are within the uncertainty range for EV8. The results of the investigation are summarized in Table II. We find the instability is predicted to occur at a T_I^V value of approximately 3.625 °C for EV5, 3.595 °C for EV7, and 3.595 °C for EV8. We note that the predicted T_I^V values are the same for EV7 and EV8 because the onset parameter depends strongly on T_I^L values in this circumstance and the values are the same for these two experiments. The dependence of the stability parameter on the input variables is shown in more detail in the parametric analysis in the following section. The onset T_I^V value for EV8, in which Marangoni convection was observed, lies within the possible range; however, the values for EV5 and EV7, which were observed to be quiescent, do not lie within the possible range. Therefore, the theory is consistent with experimental observations since it predicts that a transition to Marangoni convection is possible between EV7 and EV8.

VIII. PARAMETRIC ANALYSIS OF THE STABILITY PARAMETER

As discussed above and summarized in Eq. (78), the present stability parameter for liquids evaporating from funnels constructed of conducting materials χ_s is primarily a function of the interfacial vapor phase temperature, the interfacial liquid phase temperature, the evaporation flux, and the radius of the spherical interface. The experimental comparison indicates a strong link between these parameters and the stability. The direct effect of the parameters on the stability is investigated by performing a parametric analysis, in which each parameter is analyzed individually while the others are held constant.

The methodology for the analysis will be to use the data from the EVD5 experiment as a starting point and vary each parameter individually. The analysis was performed for a number of the experiments and the results were found to be identical, so the EVD5 experiment was selected and is representative of all of the experiments.

We emphasize that this parametric analysis is not a physically based analysis since it is not believed that the parameters can be independently varied. There is reason to believe from experimental observations [17] that there is a link between the temperature discontinuity at the interface and the evaporation flux. However, there is presently no expression describing this relationship and the result may depend on a number of factors that have not been rigorously investigated such as the thermal boundary conditions of the system, the temperature in the bulk phases, and the presence of Marangoni convection. So these parameters are varied independently, exclusively for the purpose of determining their influence on the onset of Marangoni convection.

A. Effect of interfacial vapor phase temperature

The result of varying T_I^V while holding the other variables fixed is plotted in Fig. 3. It can be seen that as T_I^V is decreased from the measured value of 4.04°C, the system becomes unstable. An interesting phenomenon is that since T_I^L is fixed in this case, as T_I^V is decreased, it approaches the value of T_I^L (3.61°C); thus, the temperature discontinuity at the interface ($\Delta T_I = T_I^V - T_I^L$) is decreasing. Therefore, the analysis indicates that as T_I^V decreases the system becomes less stable or, alternatively, as the temperature discontinuity decreases the system becomes less stable.
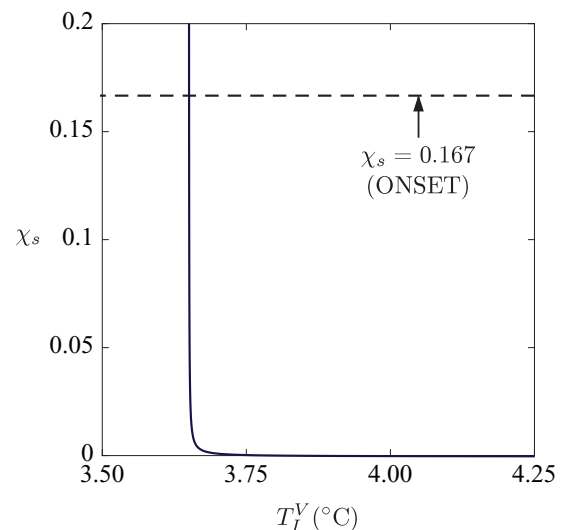

FIG. 3. (Color online) Stability parameter χ_s plotted versus T_I^V for T_I^L fixed at 3.61°C, j_{ev} at 0.221 g/m² s, and r_I at 4.4 mm.
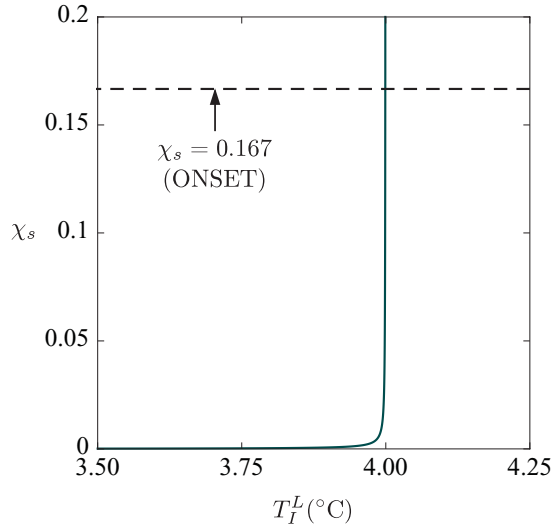
FIG. 4. (Color online) Stability parameter χ_s plotted versus T_I^L for T_I^V fixed at 4.04 °C, j_{ev} at 0.221 g/m^2 s, and r_I at 4.4 mm.

B. Effect of interfacial liquid phase temperature

The result of varying T_I^L is plotted in Fig. 4. It can be seen that as T_I^L is increased from the measured value of 3.61°C, the system becomes unstable. Similar to the T_I^V analysis, it is interesting to observe the effect of decreasing the temperature discontinuity. Since T_I^V is fixed in this case, as T_I^L is increased, it approaches the value of T_I^V (4.04 °C); thus, the temperature discontinuity at the interface is decreasing. Therefore, the analysis indicates that as T_I^L increases the system becomes less stable or, alternatively, and consistent with the T_I^V case, as the temperature discontinuity decreases the system becomes less stable.

C. Effect of evaporation flux

The result of varying j_{ev} is plotted in Fig. 5. It can be seen that as j_{ev} is increased from the measured value of 0.221 g/m^{2}s,
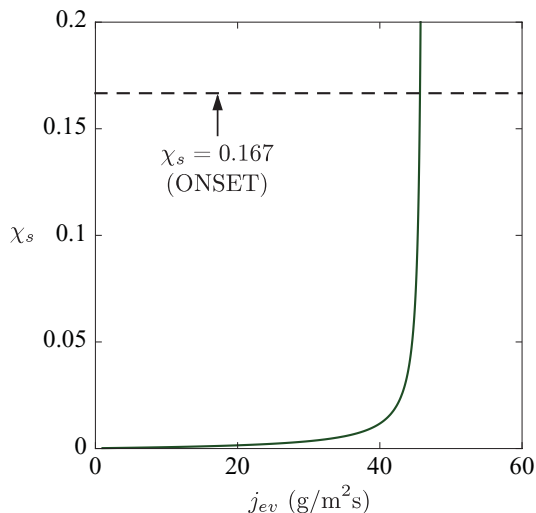

FIG. 5. (Color online) Stability parameter χ_s plotted versus j_{ev} for T_I^V fixed at 4.04 °C, T_I^L at 3.61 °C, and r_I at 4.4 mm.
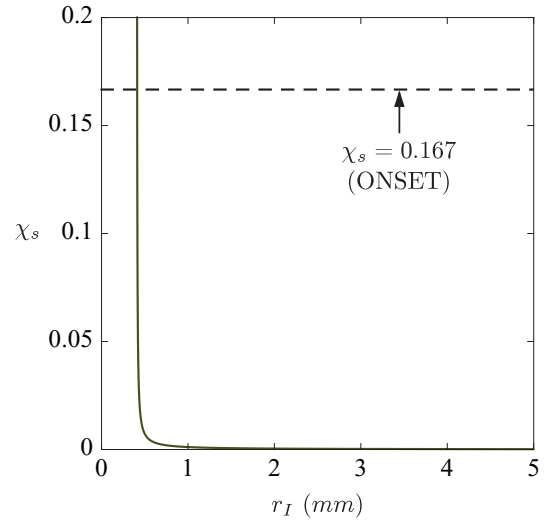

FIG. 6. (Color online) Stability parameter χ_s plotted versus r_I for T_I^V fixed at 4.04 °C, T_I^L at 3.61 °C, and j_{ev} at 0.221 g/m^2 s.

the system becomes unstable. First, this result is compatible with what would be expected physically since an instability that results from evaporation should result in a system that becomes less stable as the evaporation rate is increased. Second, from Fig. 5 it can be seen that the evaporation rate expected to yield an instability for fixed interfacial temperature values is more than two orders of magnitude higher than what was observed in the experiments.

D. Effect of the radius of a spherical interface

The result of varying r_I is plotted in Fig. 6. It can be seen that as r_I is decreased from the measured value of 4.4 mm, the system becomes unstable. This indicates that liquids evaporating from smaller funnels are less stable.

IX. CONCLUSION

A linear stability analysis has been performed for liquids evaporating from funnels constructed of either insulating or conducting materials. The theoretical results have been compared to experimental observations with D_2O and H_2O evaporating from funnels constructed of PMMA and stainless steel.

The stability analysis for liquids evaporating from funnels constructed of insulating materials predicted that there would not be a transition to Marangoni convection and the system would remain stable for all evaporation rates. The stability analysis for liquids evaporating from funnels constructed of conducting materials yielded an expression for a stability parameter comprised of only physical variables defined at the liquid-vapor interface and no fitting parameters. Therefore, we could use the parameter to generate a prediction for the onset of Marangoni convection and compare it directly with experimental observations. The differing results from these two analyses demonstrates the importance of the thermal

properties of the boundary wall on the stability of bounded systems.

The theoretical result for the insulated case correctly described the observations of quiescent (stable) evaporation in the experiments with H_2O evaporating from a funnel constructed of PMMA [4]. The stability parameter χ_s was used to calculate onset predictions for the experiments with H_2O and D_2O evaporating from a funnel constructed of stainless steel [1,2]. The predictions were consistent with the experimental observations for both liquids. The experimental data did not have the precision or range required to provide a rigorous validation of the theoretical result.

A parametric analysis was performed for the stability parameter presented herein. The analysis demonstrated that smaller interfacial temperature discontinuities, higher evaporation rates, and smaller radii correspond to less stable systems.

ACKNOWLEDGMENTS

APPENDIX: STATISTICAL RATE THEORY EXPRESSION FOR EVAPORATION FLUX

The evaporation flux is given by Refs. [17,18]

$$j_{\text{ev}} = 2mK_e \sinh\left(\frac{\Delta s_{lv}}{k_b}\right), \tag{A1}$$

where

$$K_e = \frac{\eta P_s(T_I^L)}{\sqrt{2\pi m k_b T_I^L}}, \quad \eta = \exp\left[\frac{v_f(T_I^L)}{k_b T_I^L}\left[P_e^L - P_s(T_I^L)\right]\right],$$

$$\frac{\Delta s_{lv}}{k_b} = \ln\left[\left(\frac{T_I^V}{T_I^L}\right)^4 \frac{P_s(T_I^L)}{P^V}\right] + \ln\left[\frac{q_{\text{vib}}(T_I^V)}{q_{\text{vib}}(T_I^L)}\right]$$
$$+ 4\left(1 - \frac{T_I^V}{T_I^L}\right) + \left(\frac{1}{T_I^V} - \frac{1}{T_I^L}\right)\sum_{l=1}^{3n-6}\left[\frac{\theta_l}{2} + \frac{\theta_l}{e^{\theta_l/T_I^V} - 1}\right]$$
$$+ \frac{v_f(T_I^L)}{k_b T_I^L}\left[P^V + \frac{2\gamma^{LV}(T)}{r_I} - P_s(T_I^L)\right],$$

$$\theta_l = \frac{\hbar\omega_l}{k_b}, \quad q_{\text{vib}}(T) = \prod_{l=1}^{3n-6}\frac{e^{-\theta_l/2T}}{1 - e^{-\theta_l/T}},$$

and P_e^L must satisfy

$$P_e^L - \frac{2\gamma^{LV}(T)}{r_I} = \eta P_s(T_I^L),$$

where k_b is the Boltzmann constant, $\hbar$ is the reduced Planck constant, m is the mass of a molecule undergoing evaporation, ω_l is a molecular phonon, v_f is the specific volume of the liquid at saturation, γ^{LV} is the surface tension at the liquid-vapor interface, $P_s(T_I^L)$ is the saturation pressure, and P_e^L is the liquid pressure that would exist at equilibrium. The values of the properties for H_2O are listed in Ref. [1] and those for D_2O are in Ref. [2].

[1] F. Duan and C. A. Ward, Phys. Rev. E **72**, 056302 (2005).

[2] F. Duan and C. A. Ward, Phys. Rev. E **72**, 056304 (2005).

[3] F. Duan, V. K. Badam, F. Durst, and C. A. Ward, Phys. Rev. E **72**, 056303 (2005).

[4] I. Thompson, F. Duan, and C. A. Ward, Phys. Rev. E **80**, 056308 (2009).

[5] H. Ghasemi and C. A. Ward, Phys. Rev. Lett. **105**, 136102 (2010).

[6] S. S. Anandan and V. Ramalingam, Therm. Sci. **12**, 5 (2008).

[7] M. Groll, M. Schneider, V. Sartre, M. C. Zaghdoudib, and M. Lallemand, Rev. Gen. Therm. **37**, 323 (1998).

[8] J. Kim and S. Y. S. U. Choi, Int. J. Heat Mass Transfer **47**, 3307 (2004).

[9] J. R. A. Pearson, J. Fluid Mech. **4**, 489 (1958).

[10] M. Bestehorn, Eur. Phys. J. Spec. Top. **146**, 391 (2007).

[11] K. S. Das, B. D. MacDonald, and C. A. Ward, Phys. Rev. E **81**, 036318 (2010).

[12] V. K. Badam, V. Kumar, F. Durst, and K. Danov, Exp. Therm. Fluid Sci. **32**, 276 (2007).

[13] V. M. Ha and C. L. Lai, Proc. R. Soc. London Ser. A **457**, 885 (2001).

[14] R. Liu, Q.-S. Liu, and W.-R. Hu, Chin. Phys. Lett. **22**, 402 (2005).

[15] V. M. Ha and C. L. Lai, Int. J. Heat Mass Transfer **47**, 3811 (2004).

[16] M. C. Kim, D. Y. Yoon, and E. Cho, Korean J. Chem. Eng. **26**, 1461 (2009).

[17] C. A. Ward and G. Fang, Phys. Rev. E **59**, 429 (1999).

[18] C. A. Ward, J. Non-Equilib. Thermodyn. **27**, 289 (2002).

[19] A. D. Polyanin, *Handbook of Linear Partial Differential Equations for Engineers and Scientists* (Chapman & Hall/CRC, Boca Raton, FL, 2002).